Narrow Antiadiabatic Peak in Optimally Doped and Underdoped High-T_c Superconductors

D. K. Sunko* and S. Barišić
Department of Physics, Faculty of Science, University of Zagreb,
Bijenička cesta 32, HR-10000 Zagreb, Croatia.

We study the effect of antiferromagnetic (AF) correlations in the three-band Emery model, with respect to the experimental situation in weakly underdoped and optimally doped BSCCO. In the vicinity of the vH singularity of the conduction band there appears a central peak in the middle of a pseudogap, due to an antiadiabatic quasiparticle, which is insensitive to the energy scale of the mechanism responsible for the pseudogap. We find a quantum low-temperature regime, in which the pseudogap profile is created by zero-point motion of the magnons. Detailed analysis of the spectral functions along the $(\pi, 0)$–(π, π) line shows significant agreement with experiment. We conclude that optimally doped BSCCO has a well-developed pseudogap of the order of 1000 K. This is only masked by the antiadiabatic quasiparticle, which provides the experimentally observed small binding energy scale.

I. INTRODUCTION

Angle-resolved photoemission (ARPES) measurements of electronic spectral functions of high-T_c superconductors have evolved as an important test of theoretical understanding of these materials, especially as the experimental techniques have continuously improved [1–3]. A long-standing issue in these measurements is the appearance of the pseudogap [4], observed near the vH points for underdoped systems. Experimentally, the pseudogap is clearly connected with a (π, π) correlation [3], and the most natural candidate for its origin are antiferromagnetic fluctuations above their transition point [5]. However, the underdoped state is surfeit with low-energy correlations, about whose relevance for either the pseudogap, or the superconducting mechanism itself, there is no general agreement at present. They have been interpreted as stripes [6], paramagnons [5], phonons [7], and superconducting fluctuations above T_c [8].

The present work studies the effect of dispersive antiferromagnetic paramagnons on the electronic spectral response in a simple semiphenomenological approach. We hope to use experiment to constrain the eventual theory of the optimally doped and weakly underdoped state. Using an effective weak-coupling framework, we limit ourselves to model-independent interpretations as far as possible. Our most important observation is that the pseudogap does not really disappear at optimal doping, but is instead rather inefficient at suppressing part of the spectral strength around the vH points. The unsuppressed strength appears at the Fermi level as an 'antiadiabatic' central peak in the middle of a still fairly wide and deep pseudogap. The second significant observation is that the pseudogap can appear also in a purely quantum regime, through the zero-point motion of the paramagnons. This is opposite to the usual 'textbook' pseudogap, which is in a semiclassical regime, with a nearly (but not quite) divergent magnon occupation number.

II. WEAK COUPLING IN SPIN, STRONG COUPLING IN CHARGE

Let us list at the beginning the main physical ingredients of our approach. We speak in terms of AF paramagnons, as their observed behavior fits this description most closely. The dominant perturbing correlation is centered around the AF wavevector $\mathbf{Q} = (\pi, \pi)$. The energy scale of this correlation is higher than the temperature. (We recall that the AF mode in BSCCO is at 41 meV [9].) The paramagnons are dispersive, without a low-energy component. We could include stripes fairly easily, but at present regard it as propitious that we obtain the results below already without them.

Like some other authors [10–12], we use a phenomenological weak-coupling approach to describe the effect of the paramagnons. However, the strong coupling ($U_d = \infty$) limit does enter our calculation, through a significant

*Electronic address: dks@phy.hr

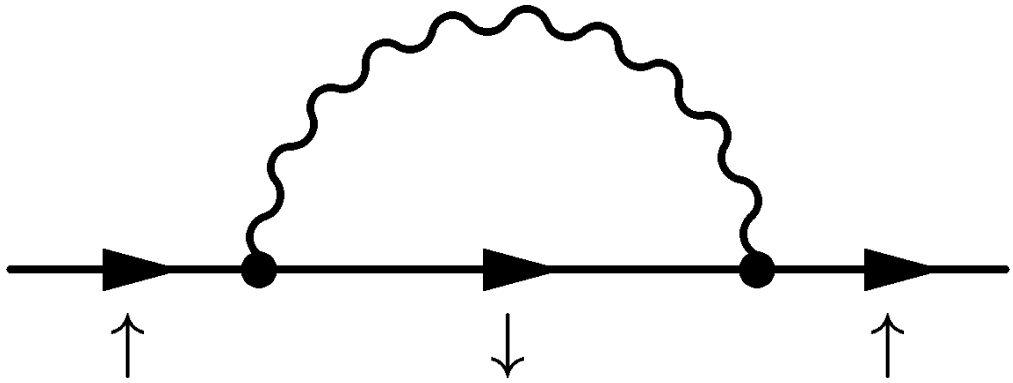

FIG. 1: Phenomenological one-magnon approximation.

renormalization of the input electronic parameters. We refer the interested reader to details published elsewhere [13–15]. Suffice it to say that we begin with a three-band (Emery) model [16], extended with a direct oxygen–oxygen hopping $t' < 0$. Strong on-site repulsion is taken into account by noting that a mean-field slave-boson calculation gives rise to an effective one-particle model in limit $|t'| > t_0^2/\Delta_{pd}$, where t_0 is the copper-oxygen hopping and Δ_{pd} the copper-oxygen energy splitting. In this regime the conduction holes contain a large oxygen component, and we take them as paramagnetic, appropriate for dopings near optimal. The input electron parametrization in this work, chosen with the above large–U regime in mind, is as follows: copper-oxygen hopping $t = 0.3$ eV, oxygen-oxygen hopping $t' = -1.$ eV, and effective copper-oxygen energy splitting $\Delta_{pf} = 3.6$ eV. The effective conduction band is then about 1 eV wide, in good agreement with data.

To justify our simple one-loop treatment of the paramagnon perturbation on the renormalized electrons, we note two things. First, there is a natural separation of the slave-boson fluctuations into fast and slow components. The latter appear static when calculating the effective dispersion of the electrons, so in fact our mean-field slave-boson renormalization of the electronic band parameters corresponds to taking this slow component into account in the charge channel [17]. The slow component in the spin channel would be relevant at small doping, where it is sometimes considered in the slave-fermion approach, but that is not the subject here. The fast component in the charge channel was shown to lead to the extended high background in both ARPES [18] and Raman [19] contexts, so again we feel free to disregard it, concentrating as we do on the pseudogap structure. Finally, the fast component in the spin channel is the paramagnon perturbation.

The second thing to note is that vertex corrections are not likely to be qualitatively important, even in a purely quantum regime. A 2D parquet calculation with $t' = 0$ was shown [20] to lead to ladder-like results ('fast parquet') in most of the space of coupling parameters, and to the marginal Fermi liquid only under very special conditions. Here we shall choose this ladder-like regime to calculate the electron self-energy Σ from Fig. 1, where the wavy line represents the spin susceptibility χ, and the vertex corrections are neglected. Hence, we concentrate entirely on the spin channel.

Having thus identified our paramagnon perturbation in the microscopic context, we proceed to treat it phenomenologically. The wavy line in Fig. 1 is taken to correspond to the simplest form of the magnetic response function,

$$\text{Im } \chi_R(\mathbf{Q}+\mathbf{q},\omega) = \frac{-2\omega_0^2\Gamma\omega}{(\omega^2-\omega_D(\mathbf{q})^2)^2+4\Gamma^2\omega^2}, \tag{1}$$

where $\mathbf{Q}$ is close to the AF wave vector (π,π), Γ is the damping, and ω_D the dispersion:

$$\omega_D(\mathbf{q})^2 = \widetilde{\omega}^2 + c^2|\mathbf{q}|^2. \tag{2}$$

Here $\widetilde{\omega}$ is the bandhead, and c the paramagnon velocity. An upper cutoff ω_0 to the magnons is also introduced, corresponding to the extension ω_0/c of the magnon anomaly around $\mathbf{Q}$.

The static magnetic structure factor related to Eqs. (1) and (2) is measured directly by elastic neutron scattering [9, 21]. It has recently been shown [22] that these experiments are consistent (in LSCO) with measurements of the nuclear spin relaxation rate T_1^{-1}, when related by the static limit of Eq. (2). A parametrization consistent with experiment is: bandhead $\widetilde{\omega} = 0.04$ eV, damping $\gamma = 0.01$ eV, cutoff $\omega_0 = 0.12$ eV, and isotropic correlation length $\xi = c/\widetilde{\omega} \sim 3$

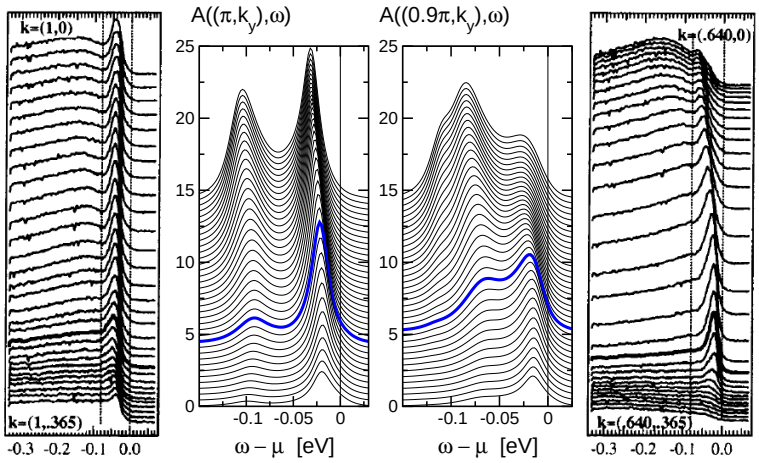

FIG. 2: Left to right: a) experimental EDC's along the X–M line, from $k_y = 0$ (top) to $k_y = 0.365\pi$ (bottom), multiplied by a Fermi function at 100 K and offset for clarity [25]. b) Calculated intensities for the same situation. c) the same for the line parallel to X–M at $k_x = 0.9\pi$. d) experiment for the line parallel to X–M at $k_x = 0.64\pi$. EDC's corresponding to the Fermi surface crossing from the maximum in the momentum distribution curve are given by a thicker line. Here $\mu = 0.025$ eV.

lattice spacings. The coupling constant, $F = 0.8$ in some dimensionless units, corresponds to a self-energy range of the order of 0.1 eV, *i.e.* about 10% of the effective $U = \infty$ hole band.

Stripes and incommensurability are widely acknowledged complications in these materials, which we do not include here. We note they correspond to slow modes in the magnon sector, *i.e.* as if our Im χ contained not only the dispersive branches, but also a low-energy component. The latter can be taken straightforwardly into account by an ansatz [23] modifying Eq. (1). However, our results indicate this is not needed to reproduce the main features of the electronic spectral structure observed by ARPES along the $(\pi, 0)$–(π, π) line. Then the only parameter left to adjust the AF dynamics in Eq. (1) is the ratio of the damping Γ and the bandhead $\widetilde{\omega}$. Magnetic fluctuations are strongly overdamped in the normal state, but as soon as superconductivity sets in, a resonance peak appears at 41 meV, around optimal doping [9, 21]. While our calculation is in the normal state, it turns out that we can obtain the superconducting ARPES profile simply by switching the paramagnon damping from overdamped ($\gamma > \widetilde{\omega}$) to underdamped ($\gamma < \widetilde{\omega}$, the values quoted above).

With respect to the electrons, the height of the paramagnon 'bandhead' $\widetilde{\omega}$ is the main physical parameter of the problem. This is due to the principal physical mechanism underlying our calculation. As already emphasized in previous work [23, 24], a special physical regime applies in the vicinity of the vH point, where the electrons themselves are slow, in fact static at the vH point itself. Then a frequency 'window' appears, of the order of the bandhead $\widetilde{\omega}$, in which a weakly damped quasiparticle survives. This creates an 'antiadiabatic' central peak in the middle of the pseudogap, as long as the paramagnon bandhead is finite.

The bandhead $\widetilde{\omega}$ also establishes the physical regime with respect to the temperature. If $kT > \widetilde{\omega}$, the system tends toward the opening of a true gap, when $\widetilde{\omega} \to 0$ *before* $kT \to 0$. This is the semiclassical (textbook) pseudogap, due to a divergence of the paramagnon occupation number. But when $kT < \widetilde{\omega}$, which is the experimental case, the electrons are only perturbed by paramagnon zero-point motion. We argue below it is this 'quantum' pseudogap which is actually observed in optimally doped BSCCO.

III. RESULTS

In Fig. 2, we show a detailed comparison with experiment for the parametrization given in the previous section. This parametrization was in fact fixed by comparison with a different experiment [2], at the $(\pi, 0)$ point alone, so Fig. 2 is a prediction of the model for the evolution of the ARPES signal in the Brillouin zone along the $(\pi, 0)$–(π, π) line and parallel to it. All the qualitative experimental features are correctly obtained: both the major and minor energy scales, and the downturn (in energy) of the antiadiabatic peak as one moves further away from the Fermi crossing. Such an approaching-then-receding of the narrow peak with respect to the Fermi level has been noticed in experiment [25], and becomes more pronounced with underdoping.

We note that the central peak is generally *not* found at the Fermi energy, except for parametrizations with high symmetry (*e.g.* vH point, $t' = 0$, and half-filling). In realistic situations, the peak moves away from the Fermi energy, producing a 'leading-edge' energy scale controlled principally by the chemical potential, affected of course by its own

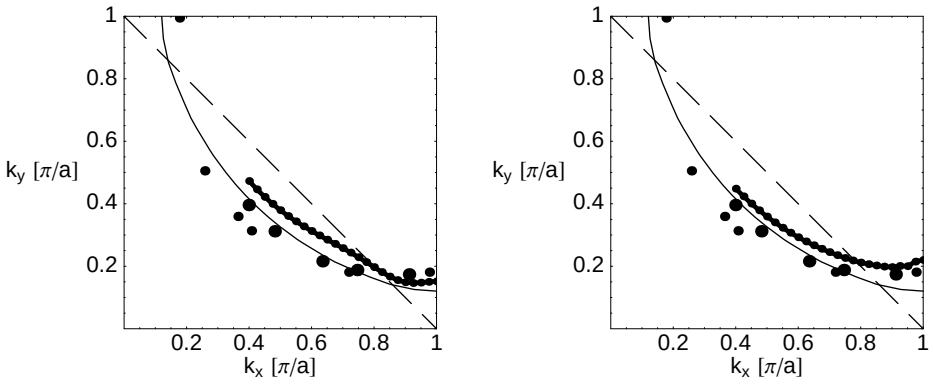

FIG. 3: Thin lines: zeroth-order $U_d = \infty$ Fermi surfaces. Points connected with thick lines: Fermi surfaces from maxima in momentum distribution curves at $\omega = \mu$. Dashed lines: zone diagonals. Left: high-temperature pseudogap, $kT = 1.0$ eV and $F = 0.03$. Right: low-temperature pseudogap. In this figure, $\mu = 0.015$ eV. Points: experimental Fermi crossings, large: Ref. [26], small: Ref. [27]. (The value of F in the high-temperature case is adjusted to give a practically identical EDC profile at the vH point as in the low-temperature case, in particular the same pseudogap scale.)

dispersion. It is unrelated to the primary AF scale, which determines the width of the pseudogap by the 'high-energy' side lobes, and is of the order of 0.1 eV in the calculation and experiment.

In the right two panels of Fig. 2, we show what happens as one moves towards the Γ point. We note a significant redistribution of spectral strength, such that the side lobe is much stronger at $k_y = 0$, the Γ–X line itself, but quickly loses strength as one moves perpendicularly away from it in the k_y direction, parallel to the X–M line. Finally at $k_y = 0.35\pi/a$, only the antiadiabatic peak survives. Experimentally, much the same behavior has been observed, with the proviso that it seems to evolve more slowly in the Γ direction, so the qualitative features we calculate around $k_x = 0.9\pi$ here are observed around $k_x = 0.65\pi$ in experiment [25]. The experimentally observed strength redistribution between the two peaks is characteristic in our calculation only of the low-temperature regime, $kT < \widetilde{\omega}$. In the high-temperature regime, the opposite occurs: the central peak loses strength before the side lobe. This is one piece of evidence that the quantum, not semiclassical, pseudogap is the one actually observed.

In Fig. 3, we show the difference between the semiclassical and quantum pseudogap regimes in their effect on the Fermi surface. In the left panel, which is in the high-temperature regime $kT > \widetilde{\omega}$, one can clearly discern the Fermi surface bending towards the zone diagonal at the 'hot spot'. The right panel is in the quantum regime $kT < \widetilde{\omega}$, and there is clearly no hot-spot effect, rather the opposite: the Fermi surface bends *away* from the zone diagonal, even with a tendency to curve upwards. While the latter tendency has never been clearly observed — there is only one experiment [27], the small points Fig. 3, which seems to show such a tendency — the former bending to follow the zone diagonal can be excluded with certainty. The Fermi surface of optimally doped BSCCO in the vicinity of the vH points is at least a straight line parallel to the Γ–X line. In other words, the observed Fermi surface differs with respect to the zeroth order $U = \infty$ shape (thin line in Fig. 3) in the way suggested by the right-hand panel in the figure, increasing the angle with the zone diagonal, rather than decreasing it as in the left panel. Thus, both the evolution of ARPES spectra in the Brillouin zone and the shape of the Fermi surface in BSCCO seem to point in the same direction, that the observed pseudogap is due to zero-point motion of the magnons.

IV. SUMMARY

In the present work, we have tried to establish the physical regime of the 'peak-dip-hump' feature observed in optimally doped and slightly underdoped superconducting BSCCO. Our interpretation has three main components.

First, the narrow feature itself is that part of the original electron spectral strength which is not suppressed by the pseudogap mechanism, because it consists of electrons which are so slow, that they average out even the slowest dispersive magnons. This opens a 'window' in the electron spectral function, of the order of the magnon bandhead $\widetilde{\omega}$, in which a weakly damped 'antiadiabatic' quasiparticle appears as a sharp and narrow peak. We find that the calculated dispersion of this peak closely follows experiment. The leading edge scale of the peak, which is the lowest binding energy in the problem, is not related to the primary AF scale, but is mainly regulated by doping.

Second, the side lobe ('hump') is given by the AF scale, about 1000 K, but through a low-temperature pseudogap

mechanism, which is due to the zero-point motion of the magnons, not to their building up a macroscopic (classical) mode. The latter, usual mechanism to obtain a pseudogap, is excluded by two pieces of evidence at present. One is that it predicts the opposite redistribution of spectral strength than the one observed (see Fig. 2), the other is that it predicts that the Fermi surface should anomalously bend towards the zone diagonal at the 'hot spot,' which is similarly not observed.

Third, we find that we can account for the difference between the normal and superconducting ARPES profiles within our normal-state calculation, simply by switching the paramagnon damping, from overdamped in the normal state to underdamped in the superconducting state. Thus it would appear that superconductivity has only an indirect effect on the spectrum, in particular the narrow feature can be obtained without relation to the superconducting mechanism.

We have so far not considered any low-energy components in the magnon response, in particular there are no (possibly incommensurate) stripes in our calculation. It may be that they will turn out to play a role in the shape and spectral composition of the side wings, but we believe such an extended calculation will not controvert the main results obtained here.

To conclude, we claim that the pseudogap in optimally doped BSCCO is in fact fully developed, of the order of 1000 K, and is only masked by the antiadiabatic quasiparticle. The small separation between the antiadiabatic peak and the Fermi level appears naturally in the calculation, and is not due to any independent physical mechanism.

[1] Z. X. Shen, W. E. Spicer, D. M. King, D. S. Dessau, and B. O. Wells, Science **267**, 343 (1995).
[2] A. V. Fedorov, T. Valla, P. D. Johnson, Q. Li, G. D. Gu, and N. Koshizuka, Phys. Rev. Lett. **82**, 2179 (1999).
[3] J. C. Campuzano, M. R. Norman, and M. Randeria, in *The Physics of Superconductors Vol. II: Novel Superconductors: Cuprate, Heavy-Fermion, and Organic Superconductors*, edited by K. H. Bennemann and J. B. Ketterson (Springer, 2004, to appear), cond-mat/0209476.
[4] M. Randeria, in *Proceedings of the International School of Physics 'Enrico Fermi' Course CXXXVI on High Temperature Superconductors*, edited by G. Iadonisi, J. R. Schrieffer, and M. L. Chiafalo (IOS Press, 1998), pp. 53–75, cond-mat/9710223.
[5] M. V. Sadovskii, Uspekhi fizicheskih nauk **171**, 539 (2001).
[6] S. A. Kivelson, I. P. Bindloss, E. Fradkin, V. Oganesyan, J. M. Tranquada, A. Kapitulnik, and C. Howald, Rev. Mod. Phys. **75**, 1201 (2003).
[7] A. Lanzara, P. V. Bogdanov, X. J. Zhou, S. A. Kellar, D. L. Feng, E. D. Lu, T. Yoshida, H. Eisaki, A. Fujimori, K. Kishio, et al., Nature **412**, 510 (2001).
[8] N. P. Ong, Y. Wang, S. Ono, Y. Ando, and S. Uchida, Ann. Phys.-Berlin **13**, 9 (2004).
[9] K. Ishida, Y. Kitaoka, K. Asayama, K. Kadowaki, and T. Mochiku, Physica C **263**, 371 (1996).
[10] A. J. Kampf and J. R. Schrieffer, J. Phys. Chem. Solids **52**, 1321 (1991).
[11] J. Friedel and M. Kohmoto, Eur. Phys. J. B **30**, 427 (2002).
[12] M. Eschrig and M. R. Norman, Phys. Rev. B **67**, 144503/1 (2003).
[13] I. Mrkonjić and S. Barišić, Eur. Phys. J. B **34**, 69 (2003).
[14] I. Mrkonjić and S. Barišić, Int. J. Mod. Phys. B **17**, 3277 (2003).
[15] I. Mrkonjić and S. Barišić, J. Supercond. **17**, 75 (2004).
[16] V. J. Emery, Phys. Rev. Lett. **58**, 2794 (1987).
[17] I. Mrkonjić and S. Barišić, Eur. Phys. J. B **34**, 441 (2003).
[18] C. A. R. S. de Melo and S. Doniach, Phys. Rev. B **41**, 6633 (1990).
[19] H. Nikšić, E. Tutiš, and S. Barišić, Physica C **241**, 247 (1995).
[20] I. E. Dzyaloshinskii and V. M. Yakovenko, Int. J. Mod. Phys. B **5**, 667 (1988).
[21] J. Rossat-Mignod, L. P. Regnault, C. Vettier, P. Burlet, J. Y. Henry, and G. Lapertot, Physica B **169**, 58 (1991).
[22] L. P. Gor'kov and G. B. Teitel'baum, *Pseudogap behavior of nuclear spin relaxation in high T_c superconductors in terms of phase separation* (2003), cond-mat/0312379.
[23] A. Bjeliš and S. Barišić, J. Physique Lett. **36**, L169 (1975).
[24] D. K. Sunko and S. Barišić, Europhys. Lett. **22**, 299 (1993).
[25] A. Kaminski, M. Randeria, J. C. Campuzano, M. R. Norman, H. Fretwell, J. Mesot, T. Sato, T. Takahashi, and K. Kadowaki, Phys. Rev. Lett. **86**, 1070 (2001).
[26] T. Valla, A. V. Fedorov, P. D. Johnson, Q. Li, G. D. Gu, and N. Koshizuka, Phys. Rev. Lett. **85**, 828 (2000).
[27] M. R. Norman, M. Randeria, H. Ding, and J. C. Campuzano, Phys. Rev. B **52**, 615 (1995).